Received: 25 August 2021 | Revised: 20 January 2022 | Accepted: 10 February 2022

DOI: 10.1002/vnl.21905

RESEARCH ARTICLE

JOURNAL OF Vinyl & Additive TECHNOLOGY WILEY

Effect of different processing techniques and presence of antioxidant on the chitosan film performance

Giulia Infurna[1,2] | Giuseppe Cavallaro[2,3] | Giuseppe Lazzara[2,3] | Stefana Milioto[2,3] | Nadka Tz. Dintcheva[1,2]

[1]Department of Engineering, University of Palermo, Palermo, Italy

[2]National Interuniversity Consortium of Materials Science and Technology (INSTM)—Research Unit of Palermo, Florence, Italy

[3]Department of Physics and Chemistry, University of Palermo, Palermo, Italy

Correspondence
Nadka Tz. Dintcheva, Department of Engineering, University of Palermo, Viale delle Scienze, Ed. 6, 90128 Palermo, Italy.
Email: nadka.dintcheva@unipa.it

Funding information
MIUR—Progetto di ricerca e sviluppo "AGM for CuHe", Grant/Award Number: ARS01_00697

Abstract

In the last two decades, the naturally occurring polysaccharides have gained great attention because of their potential applications in different sectors, for example, from food to biomedical sectors. Chitosan is a cationic polysaccharide with good transparency, and currently, it has been considered also as suitable material for the formulation film and coating in cultural heritage protection. In this work, the chitosan films (Ch), with and without natural antioxidant such as citric acid (CA), are formulated considering two different processing techniques: (i) conventional solvent casting and (ii) compression molding, that is an unconventional method for this polysaccharide, giving the possibility to formulate films with extended surface and constant thickness. The effects of processing conditions and antioxidant presence on the properties and performance are evaluated by thermo-gravimetric analysis, FTIR and UV–visible spectroscopy, water contact angle measurements and tensile test. Besides, the durability of all investigated Ch and Ch/CA has been evaluated subjecting thin film to UVB exposure and monitoring their structural changes by FTIR analysis in time. All obtained results suggest that the chitosan films can be processed successfully by both solvent casting and compression molding techniques. Further, the CA presence in Ch films has a beneficial effect on the thermal resistance and durability and no negative effect on the transparency and optical properties.

KEYWORDS

antioxidant, chitosan films, citric acid, compression molding, solvent casting

1 | INTRODUCTION

The European Commission and EU Governances underline the utmost importance of shifting towards a circular economy, with a framework of policies that make sustainable products, services, and business models.[1] However, as a part of this transition, the replacement of petroleum-based polymers by naturally occurring counterparts is imperative. In the last two decades, the production of naturally occurring polymers becomes more and more important, also due to increased public interest to environmental and human health preservation. The biopolymers include

different kinds, such as polysaccharides, polyhydroxyalkanoates, polylactic acids, starches, proteins, lipids, etc., having applications mainly in biomedical, pharmaceutical and food packaging sectors. The properties and performance of biopolymers depend on their chemical structure, molecular weight, polymerization degree, crystallinity degree and processing technologies.[2,3]

Among the biopolymers from natural sources, the most important are the polysaccharides, and they have attracted much attention thanks to their biocompatibility, biodegradability, non-toxicity and relative low cost.[4] The most abundant polysaccharide in the world, after cellulose, is the chitin, which is present widely in the exoskeleton of crustaceans, fungal cell walls and other biological materials. Therefore, by controlled MeOH deacetylation of chitin can be produced chitosan, that is a cationic polysaccharide. The chitosan is a good candidate for different applications, such as films and coatings for food preservation and conservation,[5–8] as sequestrant particles for decontamination,[9,10] in agriculture[11] and in medicine.[12–18] Since the chitosan shows a selective permeability to CO_2 and O_2[7,17] and thank to its ability to form transparent films and gels,[19,20] it is considered also as a good candidate to formulate edible coatings for some foods. As known, the chitosan is considered an excellent candidate for a controlled drug delivery and release,[12,17] and interestingly, chitosan-modified nitrocellulose membrane has been proposed as good candidate for paper-based point-of-care testing.[18] Currently, the chitosan is proposed also for cultural heritage protection,[19–23] for example, for wood,[21,22] metal and stone[19,20] consolidation and for surface cleaning.[20,23]

The chitosan properties and performance are mainly affected by grade of deacetylation,[7] presence of plasticizers[24,25] and molecular mass.[26,27] Unfortunately, the chitosan has marked water sensitivity, and this represents its main drawback, that consists in water molecules adsorption and swelling, causing mechanical and barrier properties impairment.[5,7,19] Thus, the consideration chitosan for some innovative and challenging applications can be compromised.

Concerning water sensitivity of chitosan, different crosslinking strategies have been fielded to overcome its drawback. For example, the chitosan can be crosslinked by acid treatments,[5,7] ultrasound treatment[26] and/or introduction of appropriate crosslinking agents that can interact and/or react with chitosan functionalities during film formulation.[28–35] Interestingly, some naturally occurring acids, such as ascorbic, ferulic and citric acids, are recently gained attention as good additive for chitosan, also thanks to their ability to react and stabilize polysaccharide materials.

Overall, the chitosan hydrophobicity, thermal resistance and stability, and tensile strength, can be significantly enhanced by acid and ultrasound treatments, by introduction of natural crosslinkers and/or reinforcement agent. In agreement with the literature, the naturally occurring halloysite nanotubes can be introduced in the chitosan matrix for two purposes, that is, as carrier for antioxidant molecules, improving the chitosan durability,[19] and as reinforcement agent, enhancing the chitosan stability and tensile strength.[35]

In this work, the formulation of chitosan films, containing also natural antioxidant, is carried out through two different processing techniques, specifically, a conventional solvent casting (sc) and a compression molding (cm), that is an unconventional technique for this polysaccharide material. The cm of the chitosan offers the possibility to formulate films having extended surfaces with constant thicknesses and good properties and performance, similar to those of the films formulated by sc. Therefore, the chitosan (Ch) films, with and without citric acid (CA), have been formulated by both sc and cm at the temperature of 60°C. The properties and performance of Ch and Ch/CA films, considering their potential applications for cultural heritage protection, have been accurately investigated by thermo-gravimetry analysis, FTIR and UV–visible spectroscopy, surface analysis by water contact angle (WCA) measurements and tensile test. In addition, the durability of Ch and Ch/CA films has been evaluated subjecting thin films to UVB exposure and monitoring the variations of C=O stretching of secondary amide groups and NH bending in time. All obtained results suggest that both sc and cm techniques offer the possibility to formulate films having good properties, performance and durability. The CA, being a *poly*-carboxylic acid, in Ch/CA films could exert crosslinking action, through physical or chemical interactions with chitosan functional groups.

2 | MATERIALS AND METHODS

2.1 | Materials

The materials used in this work are Chitosan (Ch), low viscosity, deacetylation degree = 75%–85% and average molecular weight = 120 kg/mol, see Schema 1A, and CA, formula

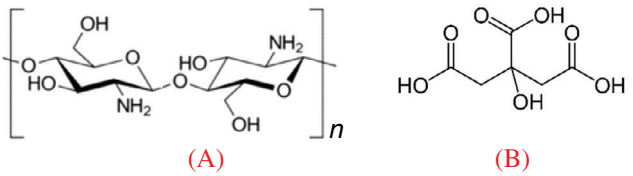

SCHEME 1 Chemical formula of (A) chitosan (Ch) and (B) citric acid (CA)

$C_6H_8O_7$, white crystals, molecular weight = 192,12 g/mol, see Schema 1B. Both chitosan (Ch) and CA have been purchased by Sigma-Aldrich and used as received.

2.2 | Film preparation

2.2.1 | Solvent casting

Chitosan at 2%wt was solved in a 3% v/v acetic acid solution, eventually an appropriate amount of CA was added to the polymer solution; the polymer solution was kept under stirring overnight. The well-dispersed mixture was poured into a glass Petri dishes under vacuum at 60°C up to 24 h in order to evaporate water solution of acetic acid until the weight was constant and to obtain films with a thickness about 100 μm. Overall CA concentration is about 2%wt.

2.2.2 | Compression molding

An aqueous acetic acid solution at 3% v/v was slowly added to Ch in powder form and manually mixed, using pestle and mortal, for 10 min. The Ch/acetic acid solution was kept constant to 25/75 wt/wt. The paste was putted into an aluminum support and located inside the molding machine at temperature of 60°C. After a preheating step of 1 min, in which no pressure was applied to the paste, a pressure ramp was applied 20–30–40 MPa for a time of 1 min at each pressure step. Then, the sample, still wet, was dried under hood to remove the rest of the solvent, resulting in a shrinkage of the film. The film thicknesses of both Ch and Ch/CA had about 100 μm. Overall CA concentration is about 2%wt.

2.3 | Characterization

2.3.1 | FT-IR

A Fourier Transform Infrared Spectrometer (Spectrum One, Perkin Elmer) was used to record IR spectra using 16 scans at a resolution of 1 cm^{-1}. Measurements were obtained from the average of triplicate samples with a calculated maximum experimental error (relative standard deviation) of around 5%.

2.3.2 | UV-visible

UV–visible Spectrometer, (Specord®250 Plus, Analytikjena, Italy), was used to record UV–Vis spectra performing eight scans between 200 and 1100 nm at a resolution of 1 nm. The transparency of the films has been evaluated through calculation of the values of linear attenuation coefficient using the formula:

$$K = 2.3 \times \frac{A_{750\,nm}}{S}, \quad (1)$$

where A is the absorbance values at 750 nm and S is the sample thickness.

2.3.3 | Thermo-gravimetric analysis

Thermo-gravimetric analysis (TGA) was carried out by using a Q5000 IR apparatus (TA Instruments) under nitrogen flow (25 cm^3/min) by heating the sample (ca. 5 mg) at the heating rate of 10°C/min from room temperature to 900°C.

2.3.4 | WCA measurement

The WCA was measured by means of an OCA 20 (Data Physics Instruments, Filderstadt, Germany) apparatus equipped with a CCD camera and a high-performance digitizing adapter. The SCA 20 software (Data Physics Instruments) was used for data acquisition. The films were fixed on top of a plane solid support and kept flat during water deposition and acquisition. The sessile drop method was used with a droplet volume of 6 μl.

2.3.5 | Mechanical characterization

Tensile tests were carried out using a Universal Testing Machine (Instron model 3365, UK), following ASTM D882 method, on rectangular samples cut by films prepared by cm and sc. The tests were performed, using tensile speed at 1 mm/min. Young's modulus (E), tensile strength (TS) and elongation at break (EB) were recorded, and the data reported represent the average values obtained by analyzing the results of eight tests per sample; the variability of mechanical tests was typically of order of ±5%.

2.4 | Photo-oxidation exposure

Photo-oxidation of Ch films, about 80 μm thick, without and with CA (at 3 wt.%), was carried out using a Q-UV-Solar Eye weatherometer (from Q-LAB, USA) equipped

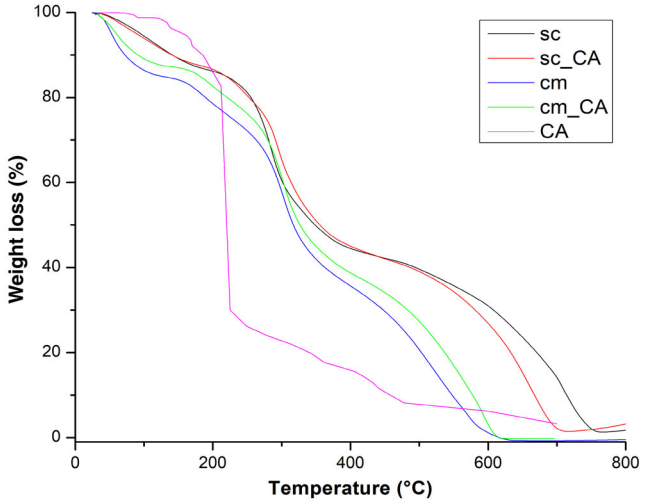

FIGURE 1 TGA curves of Ch and Ch/CA films processed by solvent casting (sc) and compression molding (cm)

with UVB lamps (340 nm). The weathering conditions were a continuous light exposure at $T = 55°C$ for 8 h and condensation at $T = 35°C$ for 4 h.

3 | RESULTS AND DISCUSSION

To evaluate the thermal resistance of the Ch and Ch/CA samples produced by sc and cm, the thermogravimetric analysis has been carried out, and in Figure 1, obtained thermograms are plotted. It is worth noting that all samples were dried for 24 h at temperature at 80°C in a vacuum oven before TGA analysis. In the temperature range between 50 and 100°C, a first weight loss is noticed for all the samples, probably due to evaluation of bonded water molecules, see the values of water content reported in Table 1. Interestingly, the amount of the coordinated water molecules results lower for the Ch and Ch/CA samples produced by sc, rather than for the samples produced by cm, see Figure 1 and Table 1. However, the drying procedures before TGA analysis is not able to totally remove the water molecules that physically or chemically interact with the chitosan chains.

Therefore, it seems that all samples are thermally stable up to ca. 250°C, then the weight losses become pronounced. Besides, the weight losses are overall about 50% than the initial ones in the temperatures between 250 and 350°C. According to literature, this could be related to random split of glycosidic bonds, releasing low molecular weight compounds and decomposing the pyranose rings through dehydration and ring-opening reactions.[35] In Table 1, the temperature values at overall weight losses at about 50% of the all investigated samples are reported and it can be noticed that sc-Ch and sc-Ch/CA samples show higher values, than the cm-Ch and cm-Ch/CA, suggesting a better thermal stability for the sc samples in this temperature range. Besides, although less pronounced, the CA presence has a beneficial effect on the Ch thermal resistance in the range 30–350°C. This could be understand considering that the CA is a polycarboxylic compound, and the CA molecules exert antioxidant action through hydrogen atoms donation at low temperature. Besides, the CA shows a significant weight loss, ca. 80%, in the temperature range 200–250°C that suggests the occurrence of CA molecules decomposition, as noticeable in Figure 1.

TABLE 1 Calculated values of temperature degradation obtained by the maximum of DTG (not shown here) and water content (%)

Sample	T (°C) at 50% weight loss	Water content (%)
sc_Ch	350.5	8.15
sc_Ch/CA	353.6	7.48
cm_Ch	309.3	14.15
cm_Ch/CA	316.7	11.50

Further pronounced weight losses for all investigated Ch samples are noticeable in the temperature interval between 450 and 600°C when the Ch sample undergo thermal decomposition associated with methane evolution and the formation of graphite-like structure. It seems that the thermal decomposition of Ch and Ch/CA samples produced by sc occurs in higher temperature intervals, that is, between 600 and 750°C, probably because the Ch chains of these samples are arranged efficiently and coordinate low amount of water molecules. Therefore, the decomposition of both sc_CA and cm_CA samples occur early then the neat Ch samples and it seems that the CA presence has a negative effect on the thermal resistance at temperature > 400°C of both sc-Ch and cm-Ch samples. The latter could be understand considering that the CA molecules decompose between 200 and 250°C, and probably, decomposed CA molecules exert a *hot-spot* action, playing a negative role on the Ch thermal resistance at high temperatures, that is, >400°C, see Figure 1.

To investigate of the structural changes of Ch-based samples, FTIR analysis is carried out, and in Figure 2a, obtained FTIR spectra are plotted. Besides, in Figure 2b, the ATR-FTIR spectrum of neat CA is also plotted. Also according to literature, in Table 2, main FTIR bands of Ch are listed.[36–38] Therefore, in Figure 2a, three main ranges, specifically, *range A* (ca. 1500–1800 cm^{-1}), *range B* (ca. 2800–3050 cm^{-1}, due to symmetric C–H stretching)

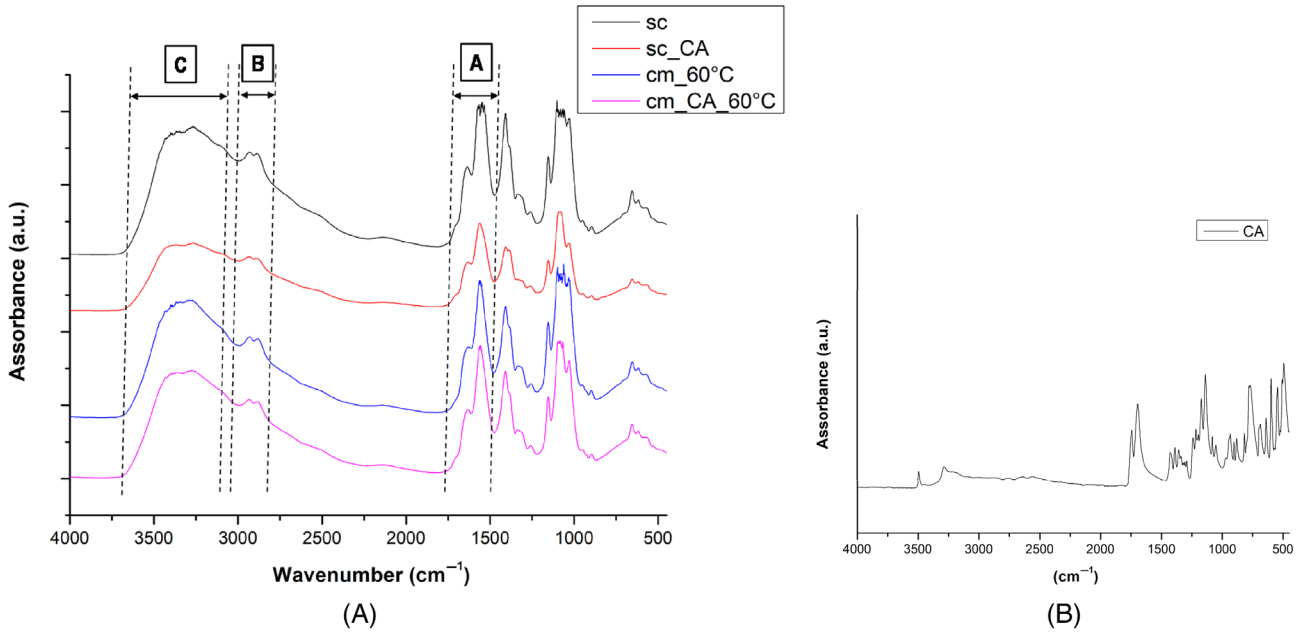

FIGURE 2 (A) FTIR spectra of Ch and Ch/CA samples processed by solvent casting (sc) and compression molding (cm) and (B) ATR-FTIR spectrum of neat CA

TABLE 2 Assignment of main IR absorption bands of Chitosan[36–38]

ν cm^{-1}	Attribution
2927	Symmetric C–H stretching
1736	>C=O stretching
1626	C=O stretching of secondary amide group (amide I)
1560 and 1530	NH_2 scissoring and N–H bending (residue of amide II)
1395	C–N stretching (amide II)
1353	N–H in plan deformation
955	Pyranose ring
890	C–N fingerprint band

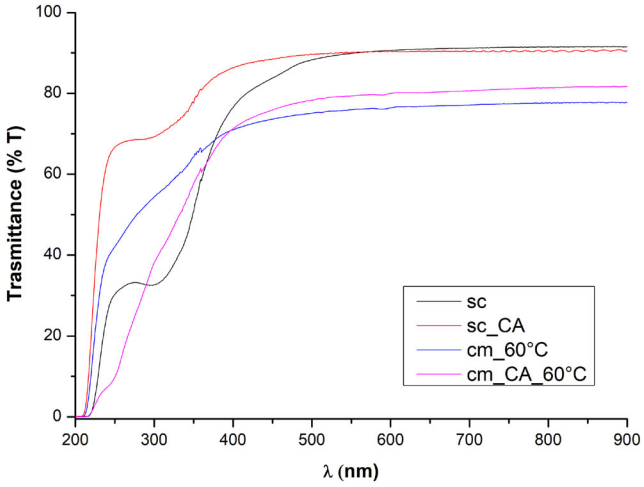

FIGURE 3 UV–visible spectra of Ch and Ch/CA films processed at 60°C by solvent casting (sc) and compression molding (cm)

and *range C* (ca. 3100–3700 cm^{-1}, due to the presence of free and bounded hydroxyl groups) are identified. In range A, two different bands appear, particularly, at ca. 1550 cm^{-1} attributed to N–H bending, ca. 1640 cm^{-1} attributed to C=O stretching of secondary amide group and a shoulder at ca. 1710 cm^{-1} attributed to >C=O stretching.

The visual inspection of the spectra in Figure 2a suggests that the CA presence does not have significant influence on the peak appearance, although the area of complex peak in range C for Ch/CA appears lower than the peak of Ch suggesting the presence of lower coordinated water molecules, also according to TGA analysis. Therefore, due to the CA presence, no additional band in the FTIR spectra of Ch is noticed and this could be understand considering the similarity of the intrinsic chemical groups of CA molecules and Ch chains. As noticeable in Figure 2b, where the ATR-FTIR spectrum of neat CA is shown, the CA shows main absorption bands in the hydroxyl range at ca. 3560 and 3290 cm^{-1}, in the carbonyl range at ca. 1721 and 1710 cm^{-1}, and other bands at ca. 1208, 1105, 779, 596 cm^{-1}, and these main bands are overlapped by the main Ch bands. Overall, by FTIR analysis, the physical interaction and/or

chemical crosslinking between the CA molecules and Ch functional groups could be only supposed.

In Figure 3, the UV–visible spectra of Ch and Ch/CA produced by both sc and cm techniques are plotted. To evaluate the film transparency in the visible range, the values of linear attenuation coefficients (K), considering the absorbance values at 750 nm and sample thicknesses and using the formula (1) in the experimental section, have been calculated, and in Table 3, obtained values are reported. Interestingly, the Ch and Ch/CA films produced by sc technique are more transparent that the Ch and Ch/CA films processed by cm technique, see Figure 3 and Table 3. Additionally, the CA presence does not negatively affect the film transparency, suggesting a beneficial effect of the antioxidant molecules on the optical properties of the Ch films produced by both sc and cm technique.

Therefore, the UV–vis spectra of sc_Ch shows a broad peak between 270 and 350 nm (peak at 294 nm), and according to literature,[39] this peak could be attributed to the oxidation of chitosan thin film during sc. As noticeable in Figure 3, the peak between 270 and 350 nm is significantly lower for sc_Ch/CA, and this could be attributed to a beneficial effect of CA presence against Ch oxidation during film formation. The UV–vis spectra of both cm_Ch and cm_Ch/CA do not show well noticeable peaks below 400 nm, probably, because the Ch oxidation for these samples occurs differently, and additionally, as discussed before, the cm samples show lower transparency in the visible domain, also due to a different organization of the molecular chains.

To investigate the surface properties of the Ch based films, WCA measurements have been carried out, and in Table 1 and Figure 4, obtained results are reported. It is noticeable that the values of contact angle measurements of sc-Ch and sc-Ch/CA are significantly lower than the values obtained for cm_Ch and cm_Ch/CA films. This result could be understand considering that the sc_Ch and sc_Ch/CA samples coordinate low amount of water molecules in comparison to the cm_Ch and cm_Ch/CA samples, as detected by TGA analysis, and subsequently, the water molecules penetration results favored. Besides, it seems that the CA presence slightly reduces Ch films hydrophobicity, probably because the well dispersed CA molecules keep the Ch chain separated, favoring the water molecules penetration.

In Figure 5, main mechanical properties, that is, Young modulus, E, tensile strength, TS, and elongation at break, EB, for all investigated samples are reported. Worth noting that the elastic modulus and tensile strength of the Ch films produced by cm result slightly higher than the values of the Ch films obtained by sc, suggesting that the compression molded films result to be more rigid than the sc films, also according to TGA and WCA measurements above commented. Interestingly, the CA presence has a beneficial effect on the ductility of sc film, supposing a better CA dispersion in sc_Ch/CA film, rather than in cm_Ch/CA one.

TABLE 3 Calculated values of linear attenuation coefficient (K) and measured water contact angles (θi) for all investigated samples

Sample	K values (mm^{-1})	θ_i (°)
sc_Ch	0.33	79.2 ± 1.10
sc_Ch/CA	0.31	74.4 ± 0.56
cm_Ch	0.61	89.2 ± 4.73
cm_Ch/CA	0.99	83.5 ± 3.60

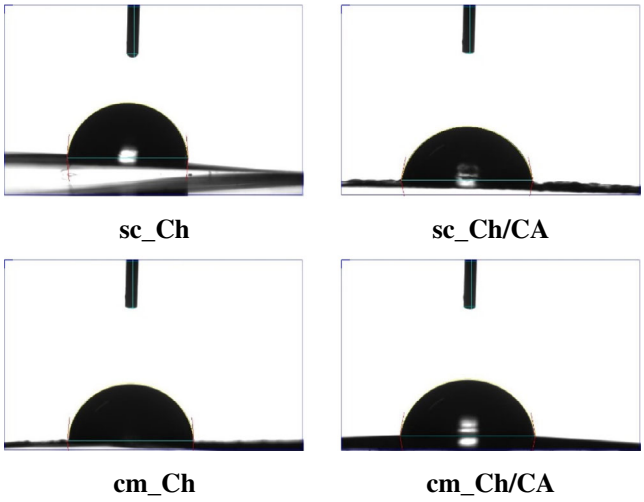

FIGURE 4 Frame of water contact angle (WCA) immediately after drop deposition on the Ch and Ch/CA films processed by solvent casting (sc) and compression molding (cm)

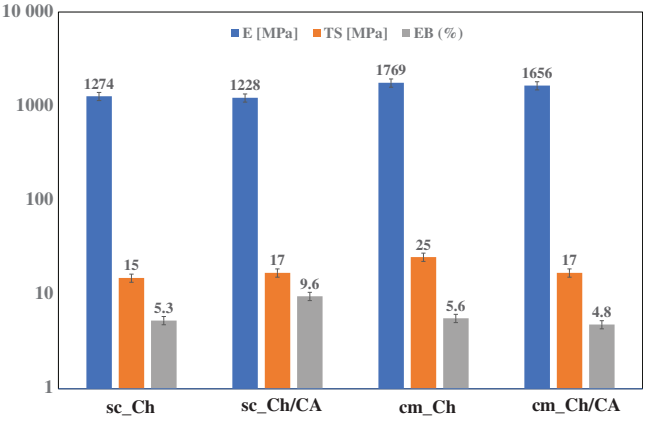

FIGURE 5 Main mechanical properties: Elastic modulus, E, tensile strength, TS and elongation at break, EB, of all investigated sample

Although limited, the presence of CA molecules has a beneficial effect on the thermal and mechanical properties on the chitosan films, without penalizing their optical transparency, that is a priority for the cultural heritage protection films. The CA, being a poly-carboxylic acid compound, could exert crosslinking action. According to literature, the CA molecules could interact with the functional groups of chitosan chains through physical and/or chemical interactions/reactions.[29,35]

To evaluate the durability of sc_Ch, sc_Ch/CA, cm_Ch and cm_Ch/CA films, thin films have been subjected to accelerated UVB exposure and the photo-oxidative degradation in time of all investigated films has been monitored through FTIR analysis at regular intervals at about 8 h. According to literature, chitosan degradation mechanism occurs mainly by depolymerization, followed by deacetylation, oxidation and interchain crosslinking,[36,37] see Figure 6A,[37] and as documented elsewhere, the photo-oxidation behavior of Ch and Ch-based systems can be profitably investigated monitoring the changes in time of the FTIR spectra in range 1750–1480 cm^{-1}, which contains three different peaks: first peak at around 1730 cm^{-1} due to >C=O stretching, second peak at around 1626 cm^{-1} due to the C=O stretching of secondary amide group (amide I) and third peak at around 1530 cm^{-1} attributed to N–H bending.[36–38] Interestingly, as currently documented by Bussiere et al.,[38] if the weathering is carried out without humidity, the chitosan film shows a remarkable photoxidation resistance, and particularly, the formation of oxygen-containing groups, that leads to arising of a peak at ca. 1700 cm^{-1}, is favored.

Therefore, all obtained FTIR spectra as a function of UVB exposure time are reported as Figures S1 and S2. It is important to note that after only 72 h of weathering all considered chitosan films become brittle, and only slight changes in the band intensities at 1626 and at 1530 cm^{-1}, that are attributed to variation of C=O stretching and NH bending, respectively, are noticed. Further, no variation in the band intensity at 1730 cm^{-1} of the chitosan films is observed during the weathering up to 72 h.

In Figure 6B,C, the at trends related to the variations of the bands at 1626 and at 1530 cm^{-1}, respectively, for

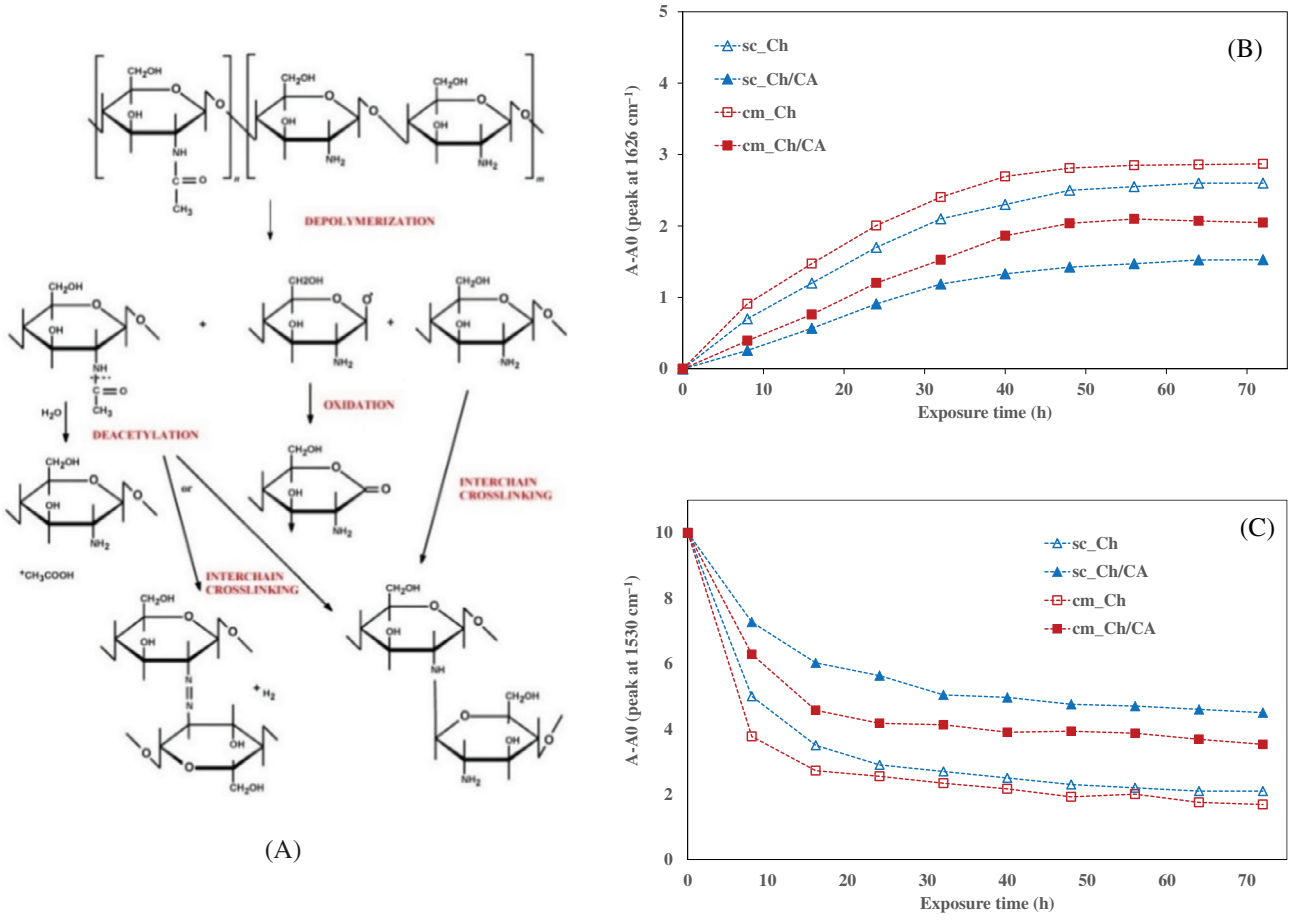

FIGURE 6 (A) Chitosan degradation mechanism[36] and variations of (B) C=O stretching of amide group (ca. 1626 cm^{-1}) and (C) NH bending (ca. 1530 cm^{-1}) for all investigated films

all investigated chitosan films as a function of exposure time are plotted. These results highlight an increase of the intensity at 1626 cm^{-1} as a function of exposure time, probably, due to a more pronounced C=O stretching vibrations, see Figure 6B, and a decrease of the intensity at 1530 cm^{-1}, due to the weakening of NH bending, see Figure 6C. These trends could be understand considering that the large amount t of intrinsic water molecules in the chitosan films and the further absorbed water molecules, that are available during condensation, can go away of the chitosan films during UVB exposure. The latter causes arising of internal forces and stresses that leads to a premature failure of the chitosan samples, and probably, this can be considered responsible for lack of oxidation evidence (no peak changes at 1730 cm^{-1}). The removal of the large amount of intrinsic and absorbed water molecules cause changes in the chitosan chain reorganization and sample premature embrittlement.

Therefore, worth noting that, due to CA presence, both peaks at 1626 and 1530 cm^{-1} are less pronounced, and this suggests that the CA molecules have a protection action for both sc_Ch and cm_Ch films. The latter could be explained considering the crosslinking action exerted by CA molecules. Although the solvent casing films show a slightly lower changes of C=O stretching vibration and weakening of NH bending, overall, it seems that the processing technique does not have a significant influence on the photo-oxidative degradation of Ch films.

4 | CONCLUSIONS

The biopolymer films, based on polysaccharides and containing natural CA, seems to be a very attractive materials also for cultural heritage protection. The chitosan films, with and without CA, have been produced by two different processing techniques at the temperature of 60°C, specifically, a conventional sc and cm, that is an unconventional processing technique for this polysaccharide material.

The Ch and Ch/CA films, produced by both sc and cm, have been characterized by thermo-gravimetry, FTIR and UV–visible spectroscopy and tensile test analyses. All obtained results suggest that the properties and performance of Ch and Ch/CA films, produced by both processing techniques, are very similar, and the latter highlights the possibility to successfully process the chitosan by cm. Therefore, the cm technique offers the possibility to produce chitosan film having large surface with constant thickness and good properties and performance. Moreover, it seems that the CA presence has a beneficial effect on the properties and performance of produced Ch films and does not have any negative effect of the film transparency.

The durability of Ch and Ch/CA films, produced by both sc and cm technique, has been investigated, and although less pronounced, the CA molecules are able to exert a protection action against the UVB exposure. Therefore, the CA, being a *poly*-carboxylic acid, in Ch/CA films could exert crosslinking action through physical or chemical interactions with the functional groups of chitosan chains.

Finally, the Ch and Ch/CA films can be successfully produced by both sc and cm techniques at the temperature of 60°C, that results to be appropriate processing temperature. The latter opens the opportunity to formulate chitosan-based films also by cm technique and these films are good candidates for cultural heritage protection.

ACKNOWLEDGMENTS

The work was financially supported by MIUR—Progetto di ricerca e sviluppo "AGM for CuHe" (ARS01_00697). Open Access Funding provided by Universita degli Studi di Palermo within the CRUI-CARE Agreement.

AUTHOR CONTRIBUTIONS

Giulia Infurna: Investigations and data curation. **Giuseppe Cavallaro:** Investigations, data curation and methodology. **Giuseppe Lazzara:** Conceptualization, methodology, supervision and writing original draft. **Stefania Milioto:** Conceptualization and supervision. **Nadka Tz. Dintcheva:** Conceptualization, methodology, supervision and writing original draft and review and editing.

DATA AVAILABILITY STATEMENT

Data sharing not applicable.

ORCID

Nadka Tz. Dintcheva https://orcid.org/0000-0003-3557-340X

REFERENCES

[1] European Commission The European Green Deal, *Eur. Comm.* **2019**, *53*, 24.
[2] C. Bastioli Ed., *Handbook of Biodegradable Polymers*, 3rd ed., Walter de Gruyter GmbH & Co KG, Shropshire, UK **2005**.
[3] A. Di Bartolo, G. Infurna, N. T. Dintcheva, *Polymers (Basel)* **2021**, *13*, 1229.
[4] S. Ebnesajjad, *Handbook of Biopolymers and Biodegradable Plastics, Properties, Processing and Applications*, 1st ed., Elsevier, Amsterdam, The Netherlands **2012**.
[5] M. N. V. Ravi Kumar, *React. Funct. Polym.* **2000**, *46*, 1.
[6] C. D. Grande-Tovar, C. Chaves-Lopez, A. Serio, C. Rossi, A. Paparella, *Trends Food Sci. Technol.* **2018**, *78*, 61.
[7] M. Z. Elsabee, E. S. Abdou, *Mater. Sci. Eng., C* **2013**, *33*, 1819.
[8] G. Cavallaro, S. Micciulla, L. Chiappisi, G. Lazzara, *J. Mater. Chem. B* **2021**, *9*, 594.

[9] R. T. De Silva, P. Pasbakhsh, K. L. Goh, S. P. Chai, H. Ismail, *Polym. Test.* **2013**, *32*, 265.
[10] S. A. Hosseini, M. Vossoughi, N. M. Mahmoodi, M. Sadrzadeh, *Appl. Clay Sci.* **2019**, *168*, 77.
[11] W. Tan, J. Zhang, Y. Mi, F. Dong, Q. Li, Z. Guo, *Int. J. Biol. Macromol.* **2020**, *165*, 1765.
[12] V. R. Sinha, A. K. Singla, S. Wadhawan, R. Kaushik, R. Kumria, K. Bansal, S. Dhawan, *Int. J. Pharm.* **2004**, *274*, 1.
[13] R. Hejazi, M. Amiji, *J. Controlled Release* **2003**, *89*, 151.
[14] L. Lisuzzo, G. Cavallaro, S. Milioto, G. Lazzara, *Polymers (Basel)* **2020**, *12*, 1.
[15] L. Lisuzzo, G. Cavallaro, S. Milioto, G. Lazzara, *New J. Chem.* **2019**, *43*, 10887.
[16] M. Liu, Y. Chang, J. Yang, Y. You, R. He, T. Chen, C. Zhou, *J. Mater. Chem. B* **2016**, *4*, 2253.
[17] E. A. Naumenko, I. D. Guryanov, R. Yendluri, Y. M. Lvov, R. F. Fakhrullin, *Nanoscale* **2016**, *8*, 7257.
[18] R. H. Tang, M. Li, L. N. Liu, S. F. Zhang, N. Alam, M. You, Y. H. Ni, Z. D. Li, *Cellulose* **2020**, *27*, 3835.
[19] G. Infurna, G. Cavallaro, G. Lazzara, S. Milioto, N. T. Dintcheva, *Polymers* **2020**, *12*, 1973. https://doi.org/10.3390/polym12091973
[20] C. Giuliani, M. Pascucci, C. Riccucci, E. Messina, M. Salzano de Luna, M. Lavorgna, G. M. Ingo, G. Di Carlo, *Prog. Org. Coat.* **2018**, *122*, 138.
[21] M. Christensen, M. Frosch, P. Jensen, U. Schnell, Y. Shashoua, O. F. Nielsen, *J. Raman Spectrosc.* **2006**, *37*, 1171.
[22] M. Broda, *Molecules* **2020**, *25*, 1.
[23] G. Cavallaro, S. Milioto, L. Nigamatzyanova, F. Akhatova, R. Fakhrullin, G. Lazzara, *ACS Appl. Nano Mater.* **2019**, *2*, 3169.
[24] M. Y. Arancibia, M. E. López-Caballero, M. C. Gómez-Guillén, M. Fernández-García, F. Fernández-Martín, P. Montero, *LWT* **2015**, *60*, 802.
[25] E. Águila-Almanza, S. S. Low, H. Hernández-Cocoletzi, A. Atonal-Sandoval, E. Rubio-Rosas, J. Violante-González, P. L. Show, *J. Environ. Chem. Eng.* **2021**, *9*, 105229. https://doi.org/10.1016/j.jece.2021.105229
[26] H. K. S. Souza, J. M. Campiña, A. M. M. Sousa, F. Silva, M. P. Gonçalves, *Food Hydrocolloids* **2013**, *31*, 227.
[27] Z. Guo, R. Xing, S. Liu, Z. Zhong, X. Ji, L. Wang, P. Li, *Carbohydr. Polym.* **2008**, *71*, 694.
[28] L. Sun, J. Sun, L. Chen, P. Niu, X. Yang, Y. Guo, *Carbohydr. Polym.* **2017**, *163*, 81.
[29] H. Wu, Y. Lei, J. Lu, R. Zhu, D. Xiao, C. Jiao, R. Xia, Z. Zhang, G. Shen, Y. Liu, S. Li, M. Li, *Food Hydrocolloids* **2019**, *97*, 105208.
[30] K. Li, J. Zhu, G. Guan, H. Wu, *Int. J. Biol. Macromol.* **2019**, *122*, 485.
[31] A. Aljawish, L. Muniglia, A. Klouj, J. Jasniewski, J. Scher, S. Desobry, *Food Hydrocolloids* **2016**, *60*, 551.
[32] E. Olsson, M. S. Hedenqvist, C. Johansson, L. Järnström, *Carbohydr. Polym.* **2013**, *94*, 765.
[33] R. Priyadarshi, B. Sauraj Kumar, Y. S. Negi, *Carbohydr. Polym.* **2018**, *195*, 329.
[34] N. T. Dintcheva, F. D'anna, *ACS Sustain. Chem. Eng.* **2019**, *7*, 12656.
[35] G. Infurna, G. Cavallaro, G. Lazzara, S. Milioto, N. T. Dintcheva, *Molecules* **2021**, *42*, 1.
[36] E. Szymańska, K. Winnicka, *Mar. Drugs* **2015**, *13*, 1819.
[37] M. Sun, T. Wang, J. Pang, X. Chen, Y. Liu, *Biomacromolecules* **2020**, *21*, 1351.
[38] P. O. Bussiere, J. L. Gardette, G. Rapp, C. Masson, S. Therias, *Carbohydr. Polym.* **2021**, *259*, 117715.
[39] J. M. Urreaga, M. U. de la Orden, *Eur. Polym. J.* **2006**, *42*, 2606.

AUTHOR BIOGRAPHIES

Giulia Infurna is PhD student at the University of Palermo, Department of Engineering and she was graduated in MSc Chemical Engineering on 22/03/2019. Currently, she is co-author of more than 10 papers.

Giuseppe Cavallaro is researcher at the University of Palermo, Department STEBICEF, and he was awarded PhD in 2014 and graduated in MSc Chemistry. He is author/co-author of more than 110 papers on indexed journals.

Giuseppe Lazzara is Associated Professor at the University of Palermo, and he was awarded PhD in 2007. His main research activities are in field of Physical-chemistry of innovative materials. He is author/co-author of more than 200 papers on indexed journals.

Stefania Milioto is Full Professor at the University of Palermo in Physical-chemistry, and she was awarded PhD in 1990. She is author/co-author of more than 200 papers on indexed journals.

Nadka Tz. Dintcheva is Associated Professor at the University of Palermo, and she was awarded PhD in 2001. Her main research activities are in the field of structure-properties-processing of innovative materials. He is author/co-author of more than 150 papers on indexed journals.

SUPPORTING INFORMATION

Additional supporting information may be found in the online version of the article at the publisher's website.

How to cite this article: G. Infurna, G. Cavallaro, G. Lazzara, S. Milioto, N. T. Dintcheva, *J. Vinyl Addit. Technol.* **2022**, *28*(2), 343. https://doi.org/10.1002/vnl.21905